DFT Studies of the Photocatalytic Properties of $BaTiO_3$ Doped with V and W for Hydrogen Production

L Phuthu[1], M Baloyi[1], T S Ranwaha[1], R S Dima[1,2] and N E Maluta[3,4]

[1]Department of Physics, University of Venda, Thohoyandou, South Africa
[2]Next Generation Enterprises and Institutions, CSIR, Pretoria, South Africa
[3]National Institute for Theoretical and Computational Sciences, Gauteng, South Africa
[4]Green Technology Confucius Institute, University of Venda, P/ Bag X 5050, Thohoyandou, 0950

E-mail: lutendo.phuthu@univen.ac.za

Abstract. The perovskite $BaTiO_3$ has been widely used as a catalyst for the synthesis of hydrogen through water splitting. However, the reaction cannot be initiated by visible light due to the large energy band gap of $BaTiO_3$. This work investigates the prospect of using the most powerful portion of solar energy, visible light, to drive the water splitting reaction. This is achieved by investigating the impact of Mono-doping and Co-doping on the electronic and optical properties of $BaTiO_3$ using first-principles density functional theory calculations. The doping elements used are Vanadium (V) and Tungsten (W). The computational were performed using the Generalized Gradient Approximation (GGA) and Local Density Approximation (LDA). The results show a reduced band gap and an increase in the optical response.

1 Introduction

The utilisation of solar radiation to perform water-splitting and make hydrogen is widely regarded as a highly advantageous method for generating clean chemical fuels, establishing renewable energy sources, and mitigating the impact of global warming and environmental concerns [1, 2]. Despite significant efforts to create sophisticated materials, the primary obstacle that persists is the reduced efficiency and selectivity for hydrogen (H_2) production using solar energy.

Among these, hydrogen production through semiconductor photocatalysis is one of the most promising pathways for producing green energy [3]. In recent years, researchers have discovered multiple productive methods to enhance the effectiveness of photocatalysis for water splitting. Commonly, precious metals such as platinum (Pt), ruthenium (Ru), rhodium (Rh), copper (Cu), silver (Ag), and gold (Au) are typically incorporated onto the surface of metal oxides to reduce the rate at which electrons and holes recombine [4]. Using the composition of semiconductors is an additional approach for harnessing visible light for hydrogen production through water splitting. When a semiconductor is connected to another semiconductor with a lower conduction band (CB) level, the electrons in the CB of the first semiconductor will go to the CB of the second semiconductor, resulting in effective separation of electrons and holes [5]. In addition, the process of cation and anion doping is highly effective in enhancing hydrogen production when exposed to visible light. This is due to its ability to shift the photo-response of a semiconductor with a broad energy band gap into the visible light spectrum. Experimental evidence has proven that pure $BaTiO_3$ can operate as a catalyst for the synthesis of hydrogen through water splitting [6, 7]. $BaTiO_3$ has a reported wide band gap of 3.2 eV, which allows for the absorption of solar light only within the ultraviolet region and no reaction in the visible light region [8]. One way to reduce the band gap

energy and increase the optical response in the visible light region is by doping $BaTiO_3$ with a foreign element. This study uses such an approach to alter the band gap of $BaTiO_3$ and increase the optical absorption activity in the visible light region. This is achieved by investigating the impact of Mono-doping on the electronic and optical properties of $BaTiO_3$ using first-principles density functional theory calculations.

2 Computational details

The geometry optimization has been performed based on the density functional theory using the generalized gradient approximation (GGA) with the Perdew-Burke-Ernzerhof (PBE) functional and norm-conserving pseudopotential implemented in the Cambridge Serial Total Energy Package (CASTEP) code on Material Studio of BIOVIA [9, 10]. The plane wave cutoff energy was set at 380 eV, and the Monkhorst-Pack scheme k-point grid sampling of Brillouin was set at 6x6x6.

3 Results

3.1 Structural Properties

A 2x2x2 supercell of $BaTiO_3$ was constructed from a unit cell. Figure 1 (a) shows the structure of a pure $BaTiO_3$ 2x2x2 supercell. Figure 1 (b) shows the structure of a doped $BaTiO_3$ 2x2x2 supercell system. The doping was done by substituting the Ti atom with either V or W. The lattice parameters of the optimized pure $BaTiO_3$ structure were calculated. The obtained lattice parameters are listed in Table 1. The results are in consistence with the experimental data as well as the theoretically calculated lattice parameter values [11, 12]. The calculated Ti-O bond length was computed as 2.084 Å and agrees with the experimental value of 2.008 Å.

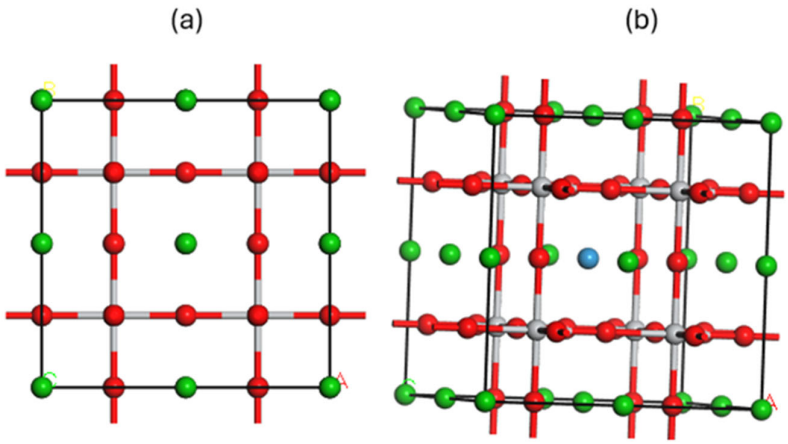

Figure 1: (a) $BaTiO_3$ 2 × 2 × 2 Supercell structure and (b) Doped $BaTiO_3$ 2 × 2 × 2 Supercell structure

Table 1: Lattice parameter of pure $BaTiO_3$

Parameters	This work	Experimental [11]	Theoretical [12]
a (Å)	4.167	3.996	4.030
b (Å)	4.167	3.996	4.030
c (Å)	4.167	3.996	4.030

3.2 Electronic Properties

To understand the electronic properties of $BaTiO_3$ structure, the band structure calculations were obtained in order to understand the energy levels that the electrons can occupy. Figure 2 (a) shows the band structure calculations of a pure $BaTiO_3$ $2 \times 2 \times 2$ supercell structure. The dotted black lines at the zero energy represent the Fermi level. The calculation shows an energy difference between the maximum valence band (MVB) and the minimum conduction band (MCB), which is the band gap as 2.219 eV. The band gap is less compared to the reported experimental value of 3.2 eV [8]. The inconsistency in this work and the reported experimental band gap is due to that the GGA calculations underestimate the band gap. However, the underestimation of the band gap does not affect the results of the rest of the calculations. Figure 2 (b) and (c) show the band structures of the V-doped $BaTiO_3$ $2 \times 2 \times 2$ supercell structure and W-doped $BaTiO_3$ 2x2x2 supercell structure, respectively. The calculations show that when $BaTiO_3$ $2 \times 2 \times 2$ supercell structure is doped with V and W, the band gap reduces to 1.345 and 0.232 eV, respectively.

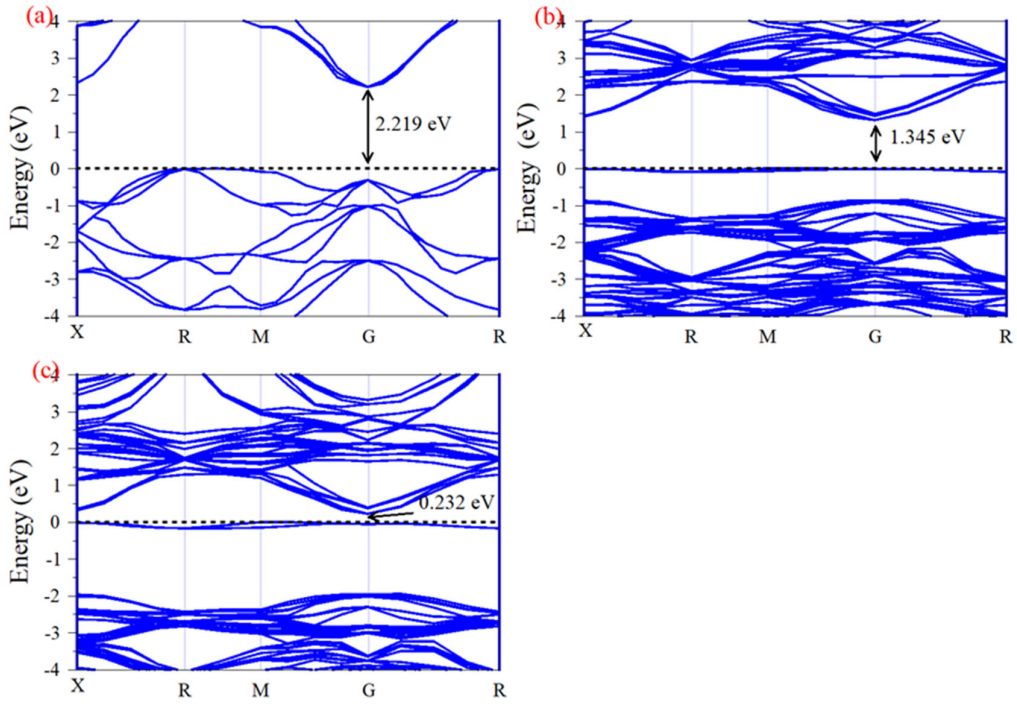

Figure 2: Calculated band structure of (a) $BaTiO_3$ $2 \times 2 \times 2$ supercell, (b) V- $BaTiO_3$ $2 \times 2 \times 2$ Supercell, and (c) W-$BaTiO_3$ $2 \times 2 \times 2$ Supercell.

To study the number of electronic states available within a specific energy range and the contribution of specific orbitals, the total density of states (TDOS) and partial density of states (PDOS) were calculated. Figure 3 (a) depicts the calculated TDOS and PDOS of the $BaTiO_3$ 2x2x2 supercell structure. The electron distribution in BaTiO3 is due to the contribution of the Ba-6s, Ti-3d, and O-2p atomic shells. It is observed that the 3d state of Ti is dominant in the conduction band (CB), while the 2p state of O is dominant in the valence band (VB). The 6s states of Ba have less contribution in the TDOS of $BaTiO_3$ 2x2x2 supercell structure. The band gap is observed in the energy range from 0.5 to 2 eV. Figure 3 (b) and (c) depict the calculated TDOS and PDOS of the doped $BaTiO_3$ 2x2x2 supercell structure. It is observed in Figures 3 (b) and (c) that the introduction of V and W introduces impurity states at the Fermi level, resulting in a reduction of the band gap.

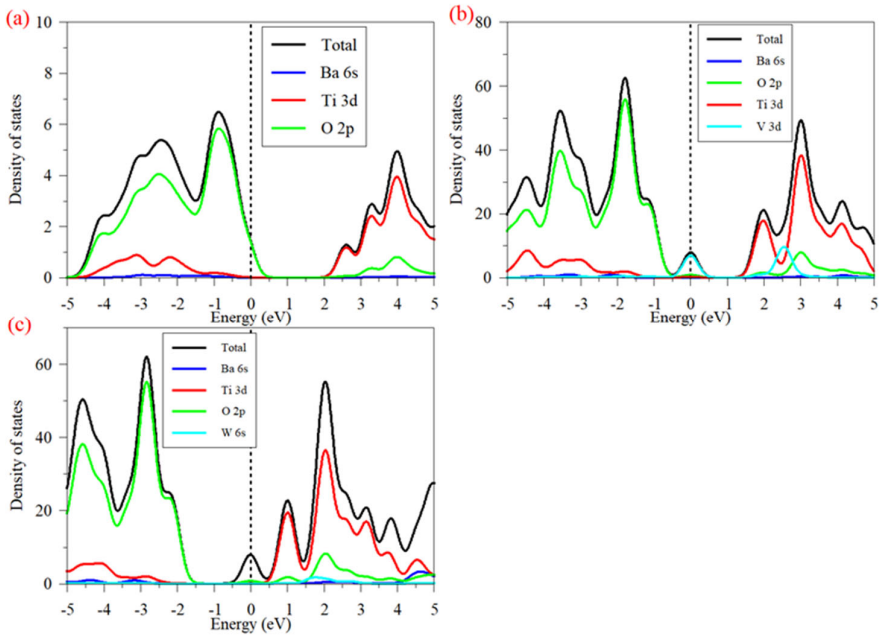

Figure 3: Calculated TDOS and PDOS of (a) $BaTiO_3$ 2 × 2 × 2 supercell, (b) V- $BaTiO_3$ 2 × 2 × 2 supercell, and (c) W-$BaTiO_3$ 2 × 2 × 2 supercell.

3.3 Optical Properties

To investigate how the $BaTiO_3$ 2x2x2 supercell structure and doped structure respond to electromagnetic radiation, particularly visible, the optical absorptions were calculated. The calculated optical absorptions are shown in Figure 4. Represented by the black curve line, the absorption curve of pure $BaTiO_3$ 2x2x2 supercell structure shows that it absorbs more in the ultraviolet region and less in the visible region. It is observed that at a wavelength of more than 600 nm of wavelength, pure $BaTiO_3$ 2x2x2 supercell structure absorption depletes. In comparison, the incorporation of V and W at the Ti sites led to a redshift in the absorption curves.

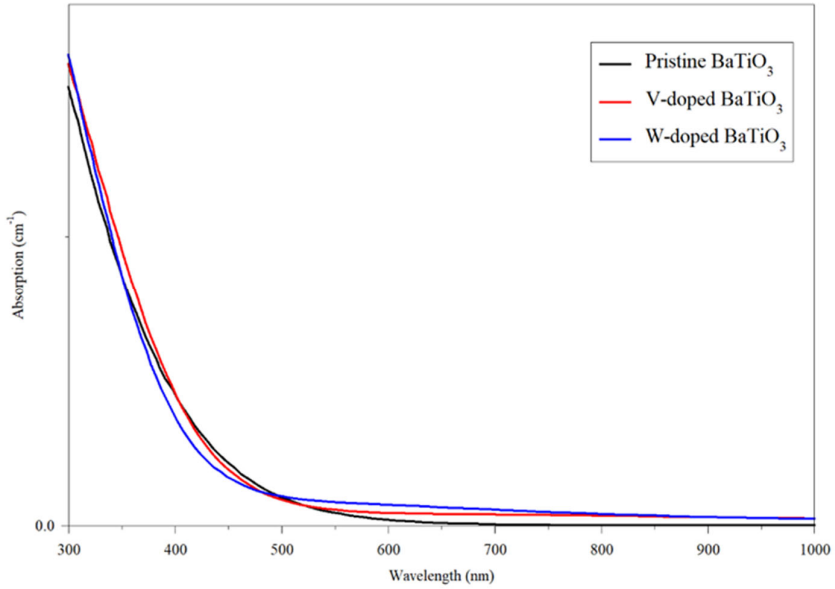

Figure 4: Optical absorption of pure and doped $BaTiO_3$ 2x2x2 supercell.

4 Conclusion

Using the first principle approach based on density functional theory, the electronic and optical properties of $BaTiO_3$ were successfully obtained. The calculated lattice parameters were compared with the literature and agreed with it. While GGA underestimated the band gap energy, it did not affect the comparison of the pure structure with the doped structure. The results show that the band gap energy of $BaTiO_3$ is reduced when $BaTiO_3$ is doped with V and W. The reduced band gap energy allows electrons to move from VB to CB with less probability of charge recombination. The density of states shows that the reduced band gap energy is due to the impurities that were induced in the Fermi energy. From the optical absorption, the dopants allow $BaTiO_3$ to have an absorption increase in the visible region. This result enables $BaTiO_3$ to be effective for water splitting.

References

[1] Boretti, A., 2022. Which thermochemical water-splitting cycle is more suitable for high-temperature concentrated solar energy?. *International Journal of Hydrogen Energy*, *47*(47), pp.20462-20474.

[2] Aravindan, M. and Kumar, P., 2023. Hydrogen towards sustainable transition: A review of production, economic, environmental impact and scaling factors. *Results in Engineering*, p.101456.

[3] Liao, C.H., Huang, C.W. and Wu, J.C., 2012. Hydrogen production from semiconductor-based photocatalysis via water splitting. *Catalysts*, *2*(4), pp.490-516.

[4] Ebrahimi, P., Kumar, A. and Khraisheh, M., 2020. A review of recent advances in water-gas shift catalysis for hydrogen production. *Emergent Materials*, *3*(6), pp.881-917.

[5] Mohammed, Y., Hafeez, H.Y., Mohammed, J., Suleiman, A.B., Ndikilar, C.E. and Idris, M.G., 2024. Hydrogen production via photocatalytic water splitting using spinel ferrite-based photocatalysts: Recent and future perspectives. *Next Energy*, *4*, p.100145.

[6] Huang, H.C., Yang, C.L., Wang, M.S. and Ma, X.G., 2019. Chalcogens doped BaTiO3 for visible light photocatalytic hydrogen production from water splitting. *Spectrochimica Acta Part A: Molecular and Biomolecular Spectroscopy*, *208*, pp.65-72.

[7] Xue, K., Jiang, Y., Mofarah, S.S., Doustkhah, E., Zhou, S., Zheng, X., Huang, S., Wang, D., Sorrell, C.C. and Koshy, P., 2023. Composition-driven morphological evolution of BaTiO3 nanowires for efficient piezocatalytic hydrogen production. *Chemosphere*, *338*, p.139337.

[8] Chen, T., Meng, J., Wu, S., Pei, J., Lin, Q., Wei, X., Li, J. and Zhang, Z., 2018. Room temperature synthesized BaTiO3 for photocatalytic hydrogen evolution. *Journal of alloys and compounds*, *754*, pp.184-189.

[9] Kresse, G. and Furthmüller, J., 1996. Efficiency of ab-initio total energy calculations for metals and semiconductors using a plane-wave basis set. *Computational materials science*, *6*(1), pp.15-50.

[10] Kresse, G. and Furthmüller, J., 1996. Efficient iterative schemes for ab initio total-energy calculations using a plane-wave basis set. *Physical review B*, *54*(16), p.11169.

[11] Gao, H., Cao, J., Liu, L. and Yang, Y., 2011. Theoretical investigation on the structure and electronic properties of barium titanate. *Journal of Molecular Structure*, *1003*(1-3), pp.75-81.

[12] Hasan, M. and Hossain, A.A., 2021. Structural, electronic and optical properties of strontium and nickel co-doped BaTiO3: A DFT based study. *Computational Condensed Matter*, *28*, p.e00578.